Article

Increase in Solubility of "Poorly-Ionizable" Pharmaceuticals by Salt Formation. A Case of Agomelatine Sulfonates.

Eliška Sko#epová, Daniel Bim, Michal Husak, Ji#í Klimeš, Argyro Chatziadi, Ludek Ridvan, Tereza Boleslavská, Josef Beránek, Pavel Šebek, and Lubomír Rulíšek

Cryst. Growth Des., **Just Accepted Manuscript** • DOI: 10.1021/acs.cgd.7b00805 • Publication Date (Web): 29 Aug 2017

Increase in Solubility of "Poorly-Ionizable" Pharmaceuticals by Salt Formation. A Case of Agomelatine Sulfonates.

Eliška Skořepová [a,b], *Daniel Bím* [e], *Michal Hušák* [b], *Jiří Klimeš* [d], *Argyro Chatziadi* [a,c], *Luděk Ridvan* [c], *Tereza Boleslavská* [c], *Josef Beránek* [c], *Pavel Šebek* [c], *Lubomír Rulíšek* [e]

[a] Department of Chemical Engineering, University of Chemistry and Technology Prague, Technicka 3, Prague 6, Czech Republic

[b] Department of Solid State Chemistry, University of Chemistry and Technology Prague, Technicka 5, Prague 6, Czech Republic

[c] Zentiva k.s., U Kabelovny 130, Prague 10, Czech Republic

[d] Department of Chemical Physics and Optics, Faculty of Mathematics and Physics, Charles University, Ke Karlovu 3, CZ-12116 Prague 2, Czech Republic

[e] Institute of Organic Chemistry and Biochemistry, Czech Academy of Sciences, Flemingovo náměstí 2, 166 10 Prague 6, Czech Republic.

eliska.skorepova@vscht.cz

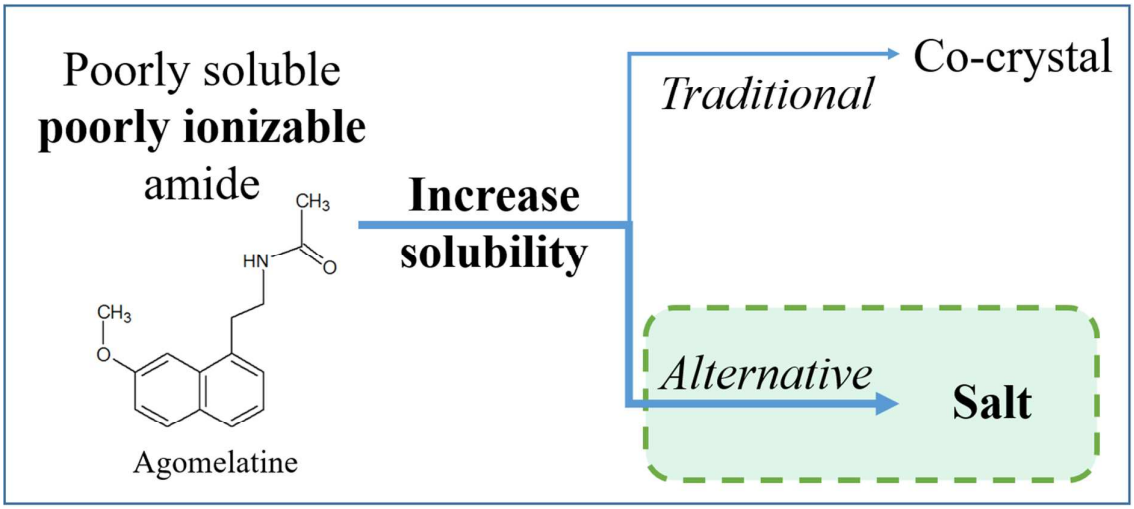

ABSTRACT

The search for new solid forms of an active pharmaceutical ingredient (API) is an important step in drug development. Often, an API has a low water solubility, which then leads to low oral bioavailability. For basic or acidic APIs, the rational solution is the preparation of salts. For neutral, 'poorly-ionizable', compounds, the co-crystallization is often the only choice. Agomelatine, a poorly soluble 'non-ionizable' amide acting as a melatonergic antidepressant is a typical representative of such class of compounds. Until recently, the only multicomponent forms of agomelatine were co-crystals. In this work, we report the preparation of three salts of agomelatine (hydrogensulfate, mesylate and besylate) and their solvated forms, along with their crystallographic characterization. Interestingly, the crystal structures of the solvated and non-solvated hydrogensulfates were determined from the same crystal via *a topotactic* transformation. In all of the structures, the agomelatine molecule was positively charged with the amide oxygen being protonated. The salt formation was also confirmed by solid state NMR measurements and DFT calculations. By sulfonate salt formation, up to ~200-times faster dissolution of agomelatine was achieved, which proves that salts might be an attractive alternative even for the poorly-ionizable compounds.

1 INTRODUCTION

The solid state chemistry is an integral part of the development of new pharmaceuticals, since different solid forms, such as polymorphs, solvates, salts or co-crystals, have different physico-chemical properties.[1] These may include hygroscopicity, stability or filterability, but the prime pharmaceutical interest are the dissolution properties.[2,3] As the number of low solubility compounds increases among the newly developed active pharmaceutical ingredients (APIs) there is an increasing interest to discover new ways to improve their dissolution properties.

Solubility and dissolution can be increased by various approaches, e.g. by micronization or by preparation of solid dispersions[4], but the method of first choice is the modification of the solid form by crystal engineering. Salt formation is the obvious route for ionizable compounds, i.e. those, which contain basic or acidic functional groups.[5] For neutral (poorly-ionizable) compounds, co-crystallization represents the alternative approach.[6]

In general, owing to their ionic character, salts would be expected to have superior dissolution and solubility properties in a polar medium. It has been reported that salts can increase the solubility up to 2000-times (delveridine mesylate[7]), whereas co-crystals usually improve the solubility only moderately[8]. For example, in the case of seven various carbamazepine co-crystals, the solubility was increased 2-152 times[9]. However, more recent studies comparing both salt and co-crystal solubilities proved that such trend is rather not universal. In the case of clotrimazole[10], five salts and two co-crystals were described and the average solubility increase was 8.68 for salts and 5.0 for co-crystals. For sildenafil[11], the average solubility increase for its five salts was 1.24 and an average of 1.48 for its four co-crystals, respectively. Finally, eight salts of niclosamide increased solubility by factor of 1.63 in average, while its only one described co-crystal increased solubility by factor of 2.46.[12] Even though the number of examples given here cannot be considered as exhaustive, it clearly demonstrates that improvement of solubility properties by salt and co-crystal formation can be in some cases comparable.

One of the excellent examples of the poorly-ionizable compounds is agomelatine (AG, Figure 1), an active pharmaceutical ingredient used for the treatment of major depressions, first synthetized by Servier in late early 90's.[13] Agomelatine's agonistic activity on MT_1 and MT_2 melatonin receptors and antagonism at the 5-HT_{2C} serotonin receptors was soon recognized as the reason of its effectiveness as an antidepressant.[14–16] It also exhibits anxiolytic effects.[17] Agomelatine was also studied with respect to treatment of manic

psychosis, Alzheimer's disease and generalized anxiety disorder.[18] It was approved by the European Medicines Agency for the treatment of major depressive episodes in 2009. In the same year, it was approved in Canada and a year later in South America, Australia and other countries. In contrast, in the United States of America, the drug has not yet been approved for marketing by the US Food and Drug Administration (FDA). Agomelatine is marketed under the names of Valdoxan or Thymanax and it is available in the form of film-coated tablets (25 mg dose).

Up to date, a number of crystal phases of agomelatine have been reported and 18 crystal structures were published. Four are the structures of the polymorphs of the pure API (polymorphs I[19], II[20], III[20] and X[21]; polymorph II is thermodynamically the most stable one[21]), 11 of them belong to co-crystals (ethyleneglycol[20], urea[22], glycolic acid[22], isonicotinamide[22], methyl-4-hydroxybenzoate[22], oxalic acid[23], pyruvic acid[23] and two polymorphs of co-crystal with hydroquinone[23] and with acetic acid[20,23]), whereas three are the structurally different iodides[24] previously published by our group.

Despite the fact that some amidic salts have already been described, the amide functional group is still frequently considered as rather non-ionizable (or poorly ionizable).[25] Only very few of already reported amidic compounds in solid forms exist as salts (0.3% occurrence in CSD)[24].

Such compounds are mostly found in their neutral state and their ionization is difficult. Compound is in general considered as 'non-ionizable' or 'poorly ionizable', when it does not contain functional groups with pK_a in the range of 2-12.[26] The pK_a of amides is between 20-25 and the pK_a of the conjugate acid is around -1.[27]

Until now, only very few pharmaceutically relevant neutral compounds have been characterized as salts. Two (rare) examples may include carbamazepine[28] or dutasteride[29]. However, to the best of our knowledge, no data regarding the solubility of the

pharmaceutically relevant amidic salts were published. This concerns also our previous work reporting on the pharmaceutically not highly relevant iodide salts of agomelatine[24], in which their solubility was *not* studied.

To extend the general knowledge in this area, agomelatine was crystallized with three sulfonic acids (sulfuric, methanesulfonic and benzenesulfonic). Based on their strength, both co-crystal and salt formation should be possible in practice. Quite unexpectedly, we observed the exclusive formation of ionic solids. The five novel crystalline forms were prepared (AG hydrogensulfate, AG hydrogensulfate methanol solvate hemihydrate, AG mesylate, AG mesylate monohydrate and AG besylate) and were characterized by single-crystal X-ray diffraction, powder X-ray diffraction, DSC and intrinsic dissolution rate. Last but not least, our extensive structural and physico-chemical characterization of the compounds is further complemented by the quantum chemical calculations; the methodology presented here might be used as efficient predictive tool in design of salts and co-crystals of the APIs.

2 EXPERIMENTAL

Materials. Agomelatine (AG, Figure 1), {N-[2-(7-methoxy-naphthalen-1-yl)ethyl]acetamide}, $C_{15}H_{17}NO_2$, is a white solid. The material was provided by Zentiva, k.s., as polymorphs I and II. The acids used for the preparation of agomelatine salts (Figure 1) and all solvents in p.a. quality were purchased from Sigma-Aldrich and were used as received.

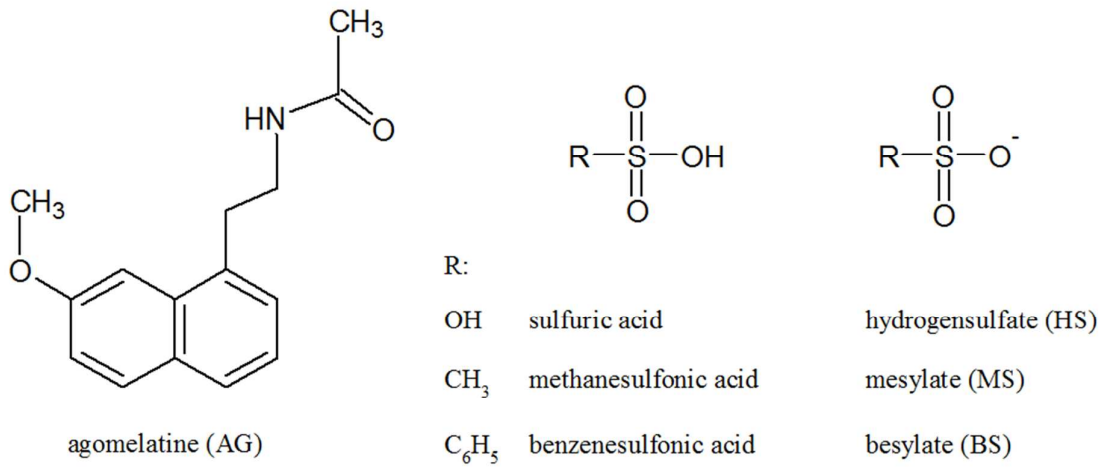

Figure 1 Molecular formula of agomelatine, the acids used and their respective anions

Sample preparation. The hydrogensulfate, mesylate and besylate salts of agomelatine were prepared by precipitation. Agomelatine was dissolved in ethyl acetate (a non-polar solvent) at 70 °C. The solution was cooled to r.t. and an equimolar amount of the corresponding acid (dissolved in a small amount of methanol, when necessary) was added drop-wise. Then, the solution was cooled to 0 °C and the precipitate filtered and dried. In this way, 'bulk' powder samples of the non-solvated forms of all three salts were prepared.

In order to prepare single-crystals, the materials were recrystallized in various ways. High-quality single-crystals of only one of the salts (AG besylate) could be prepared without major difficulties.

AG besylate (AG-BS): Agomelatine was dissolved in the excess of ethyl acetate at elevated temperature and then the equimolar amount of benzenesulfonic acid dissolved in a small amount of methanol was added. The solution was allowed to cool spontaneously and crystallize in an open vial. After several days at RT, prism-like single-crystals were obtained.

AG hydrogensulfate methanol solvate hemihydrate (AG-HS-I): The pre-prepared powder AG-HS was dissolved in methanol at elevated temperature and then the sample was cooled to (-

5) °C. After several days at this temperature in an open vial, needle-like single-crystals were obtained.

AG hydrogensulfate ansolvate (AG-HS-II): After the diffraction experiment of AG-HS-I, the single-crystal was desolvated during three days in r.t. The crystal turned white and lost its transparency, but diffracted reasonably well.

AG mesylate monohydrate (AG-MS-I): The pre-prepared powder AG-MS was dissolved in water – methanol (1:1) mixture at elevated temperature and then the sample was cooled to -5 °C . After several days at this temperature in an open vial, tile-like single-crystals were obtained.

Single-crystal X-ray diffraction. A suitable single-crystal was glued to a capillary and mounted on the goniometer. CuK$\alpha_{1,2}$ diffraction data were collected on Xcalibur PX. Data collection, cell refinement and data reduction was done by CrysAlisPro CCD[30] For structure solution, SIR92[31] and Superflip[32] were used. Programs CRYSTALS[33], Jana2006[34] and Platon[35] were used to refine structure and analyze absolute structure. Twin laws were searched for by ROTAX[36]. Direct methods were used to solve the structure; the positional and anisotropic thermal parameters of all non-hydrogen atoms were refined. The hydrogen atoms were located in a Fourier difference map, but those attached to carbon atoms were repositioned geometrically. The hydrogen atoms were initially refined with soft restraints on the bond lengths and angles to regularize their geometry (C-H in the range 0.93-0.98 Å, N-H to value of 0.86 Å, O-H to value of 0.82 Å) and Uiso(H) (in the range 1.2-1.5 times Ueq of the parent atom). Then, the hydrogen positions were refined as riding. Molecular graphics were prepared in Mercury[37] and Discovery Studio[38].

X-Ray Powder Diffraction. To perform initial analysis, a Philips X'PERT PRO MPD PANalytical diffractometer with CuK$\alpha_{1,2}$ radiation (wavelength 1.54180 Å) was used at 40 kV and 30 mA. The samples were scanned at a range 4 - 40° 2Θ with a step size of 0.017° 2Θ

and a step time of 21.32s. The results were analyzed using X'PERT HighScore Plus software[39].

To solve the structure of agomelatine mesylate anhydrate (AG-MS-II), the measurement was done on PANalytical Empyrean powder diffractometer from 6° to 60° 2Θ with CuK$\alpha_{1,2}$ radiation. The step size was set to 0.013° 2Θ and the sample was placed in a rotating capillary. PIXcel-3D area detector was used for the intensity measurement. The structure solution was done in DASH 3.2 software[40]. For the solution procedure, the CuKα_2 contribution was striped in HighScore Plus software[39] , the peak position was determined in DASH 3.2 and the indexation was done by DICVOL06[41]. For the structure solution, the structure of AG mesylate monohydrate (AG-MS-I) was used as the starting model. The problem was relatively simple (17 DOF) and, from 100 structure solution runs, 43 runs converged to the same solution. Rigid body Rietveld refinement of molecular positions and torsion angles was done in DASH 3.2. Final lattice parameters and peak shape Rietveld refinement was done by X'PERT HighScore Plus software[39]. The final Rietveld fit can be seen in Figure S1 in the Supporting information.

DFT optimization. The XRPD structure of agomelatine mesylate anhydrate (AG-MS-II) was verified by the periodic DFT-D geometry optimization using the CASTEP[42] program, GGA PBE functional, TS dispersion correction, k-point grid 48x48x48, , and the energy cut-off of 550 eV and the convergence criteria on energy of 0.00001 eV, max. force of 0.03 eV/ Å, max. displacement of 0.001 Å and max. stress of 0.05 GPa.

All structures were also optimized as isolated (solvated) systems employing Turbomole 6.6 program, BP86 functional along with def-TZVP basis set, empirical zero-damping correction to dispersion (denoted as +D3), and implicit conductor-like screening model (COSMO) with ε = 80.0 for aqueous environment or ε = 6.0 for ethyl acetate. For each compound, neutral, '*O*-

protonated' and '*N*-protonated' AG were investigated. The free energies were evaluated as follows:

$$G = E_{el} + [E_{ZPVE} + RT - RTlnQ] + G_{solv},$$

where the E_{el} is the *in vacuo* molecular (potential) energy of the system, calculated as a single-point energy (def2-TZVPD basis set) at the PBE+D3/def-TZVP equilibrium geometry; the $[E_{ZPVE} + RT - RTlnQ]$ terms were obtained from frequency calculations using the rigid-rotor/harmonic-oscillator approximation (for T = 298.15 K and p = 1 atm) whereas the solvation energy G_{solv} was calculated using conductor-like screening model for real solvents (COSMO-RS) utilizing FINE grid for cavity construction and BP_TZVPD_FINE_C30_1501.ctd parameter file. The COSMO-RS calculations were carried out on top of BP86/def2-TZVPD/COSMO($\varepsilon = \infty$) single points and G_{solv} was determined as $(E_{COSMO,inf} - E_{in\ vacuo}) + \mu_{\text{COSMO-RS}}$, where μ is the COSMO-RS chemical potential. All DFT calculations (BP86 and PBE) were expedited by expanding the Coulomb integrals in an auxiliary basis set, the resolution-of-identity (RI-J) approximation.

For the purpose of determination of the protonation site of AG amide bond, the pK_a of '*O*-protonated' AG and the pK_a of '*N*-protonated' AG were calculated according to equation:

$$pK_a = \frac{G(AG_{neutral}) - G(AG_{prot}) + G_{solv}(H^+)}{RT \cdot ln(10)},$$

where $G(AG_{neutral})$ and $G(AG_{prot})$ are the free energies of neutral AG and '*O- or N*-protonated' AG respectively; $G_{solv}(H^+)$ is the solvation energy of proton in aqueous solution (the value of -265.9 kcal/mol was used)[43]. The atomic coordinates of all optimized structures can be found in the Supporting information.

The proton transfer pathways in the crystalline phase were obtained using the Vienna Ab-initio Simulation Package (VASP) code, version 5.2.[44,45] Standard projector-augmented wave potentials were used with plane-wave basis-set cut-off set to 400~eV. *K*-point sets were chosen so that the effective supercell side length was at least 18 Å. The Perdew-Burke-

Ernzerhof exchange-correlation functional was used.[46] The dispersion corrections of Grimme and coworkers with Becke-Johson damping were added to improve the accuracy of description of intermolecular interactions.[47,48] The structures were first optimized until all forces were smaller than 0.015 eV/Å. To make the potential energy scan the hydrogen atom (proton) was gradually moved in steps towards the carbonyl oxygen. After each step, a subsequent optimization was performed, in which all the atoms, apart from the oxygen of the O_{AG} group, were allowed to move. Moreover, the hydrogen was only allowed to move in the coordinates approximately perpendicular to the $O_{AG}...O_{acid}$ line. The optimized structures, input files, final energies and scripts used for the calculations) can be found in the Supporting information.

Solution NMR. Solution NMR was used to determine the chemical purity of the prepared material and the stoichiometry. Samples were dissolved in d6-DMSO and ^{1}H and/or ^{13}C NMR spectra were measured by Bruker Avance III™ 500 MHz NMR spectrometer equipped with Prodigy probe and with repetition delay of 10s.

Solid State NMR. Solid state NMR was used to provide the phase identification and purity of the prepared materials and also to study the protonation state of agomelatine. ^{13}C and ^{15}N CP/MAS NMR spectra were measured by Bruker Avance III™ 400 MHz WB (wide bore) NMR spectrometer equipped with 4 mm probe and with 13 kHz spinning.

Differential Scanning Calorimetry. DSC measurements were performed on the DSC 131 (Setaram, France). The sample was weighed in the aluminum pan (120 μL), covered and measured in the flow of the argon gas (7.5 ml/min). The investigation was performed in the temperature range from 20 °C to 250 °C with the heating rate of 10 °C/min. The peak maximum temperature (T_m) was specified in the DSC result.

Dissolution. Dissolution properties of prepared materials were characterized using intrinsic dissolution rate (IDR) measurement. IDR describes how fast different solid phases release a molecule from the crystal lattice into a solution while the influence of particle size is eliminated. IDR were determined using Sirius inForm (Sirius Analytical, Forest Row, UK). Disc compacts were prepared by compressing approximately 40 mg of material in a 6 mm diameter dye under a constant load of 120 kg maintained for 2 minutes. Measurements were performed using 40 mL of solution at constant pH 2.0 and ionic strength of 160 mM adjusted by sodium chloride and hydrochloric acid. UV spectra were recorded each 30 seconds. Absorbance values between wavelength 250 and 350 nm were used to evaluate the amount released at a given time point. IDR was calculated using zero order linear fit through the experimental data. Only anhydrous salts were measured. All measurements were performed in duplicate.

3 Results and Discussion

3.1 X- Ray Crystallography.

By a crystallization of agomelatine with sulfuric, methanesulfonic and benzenesulfonic acids, five novel crystalline forms were prepared and their three-dimensional structures were solved. They included solvated and desolvated AG hydrogensulfate, hydrated and dehydrated AG mesylate and AG besylate. All structures but AG mesylate anhydrate were solved from single-crystal X-ray diffraction data. AG mesylate anhydrate was solved from powder data. Details of the structure solution and refinement can be found in Table 1 and will be discussed further, separately for each crystalline salt.

Table 1 Crystallographic data

	Agomelatine hydrogensulfate	Agomelatine hydrogensulfate	Agomelatine mesylate	Agomelatine mesylate	Agomelatine besylate

	methanol solvate hemihydrate		monohydrate		
form	AG-HS-I	AG-HS-II	AG-MS-I	AG-MS-II	AG-BS
formula	$C_{15}H_{18}NO_2$. HSO_4 . CH_4O_2 . $0.5H_2O$	$C_{15}H_{18}NO_2$. HSO_4	$C_{15}H_{18}NO_2$. CH_3SO_3 . H_2O	$C_{15}H_{18}NO_2$. CH_3SO_3	$C_{15}H_{18}NO_2$. $C_6H_5SO_3$
formula wt	382.44	341.38	357.43	339.41	401.48
color	colorless	white	colorless	white	colorless
cryst. morphology	needle	needle	rod	powder	plate
cryst. size (mm)	0.13 x 0.18 x 0.81	0.13 x 0.18 x 0.81	0.18 x 0.24 x 0.99	-	0.10 x 0.26 x 0.50
temp. (K)	180	180	200	293	190
radiation	Cu Kα	Cu Kα	Cu Kα	Cu Kα	Cu Kα
wavelength (Å)	1.54184	1.54184	1.54184	1.54184	1.54184
cryst. system	Triclinic	Monoclinic	Triclinic	Monoclinic	Orthorhombic
space group	$P\ \bar{1}$	$P\ 2_1$	P $\bar{1}$	$P\ 2_1/c$	$P\ 2_12_12_1$
a (Å)	7.0867(3)	8.9755(3)	9.1542(4)	12.2894(3)	8.0517(4)
b (Å)	12.9576(5)	7.1283(3)	9.4378(4)	15.1147(5)	8.4807(3)
c (Å)	20.2964(8)	12.4593(5)	11.7447(4)	9.0056(2)	28.7902(10)
α (deg)	87.206(3)	90	82.588(3)	90	90
β (deg)	87.532(3)	93.713(4)	67.490(4)	97.454(1)	90
γ(deg)	87.370(3)	90	72.856(4)	90	90
volume ($Å^3$)	1858.02(13)	795.48(5)	895.58(7)	1658.66	1965.91(14)
Z	4	2	2	4	4
density (g/mL)	1.367	1.425	1.325	1.359	1.356
no. unique reflns	12672	4868	15063	-	5999
no. obs. reflns	6493	2495	3697	-	3410
no. of params	515	217	229	-	261
$R_{\_all}$, wR_{2_all}	0.0509, 0.1098	0.0462, 0.1113	0.0673, 0.1526	Rp = 0.0538 Rwp = 0.0715	0.0438, 0.1103
$R_{\_obs}$, wR_{2_obs}	0.0422, 0.1014	0.0420, 0.1026	0.0566, 0.1360	-	0.0411, 0.1047
$\Delta\rho_{min}$, $\Delta\rho_{max}$ (e $Å^{-3}$)	-0.41, 0.39	-0.35, 0.22	-0.44, 0.44	-	-0.34, 0.24
GOF	0.9795	0.8845	0.9323	-	0.9752
CCDC number	1545354	1545355	1545356	1545357	1545353

Agomelatine Hydrogensulfates.

Crystallizing AG with sulfuric acid in ethyl acetate, AG hydrogensulfate (AG-HS) is readily formed. However, the single-crystal growth turned out to be particularly challenging since the only high-quality single-crystal did not correspond to the starting AG-HS (Figure 3 - d), but the MeOH solvate hemihydrate (AG-HS-I) was formed instead. After a subsequent desolvation - without a significant loss of single-crystal quality - the second diffraction

experiment was carried out. The new structure corresponded to the desired AG hydrogensulfate ansolvate (AG-HS-II, Figure 2 and Figure 3 - h).

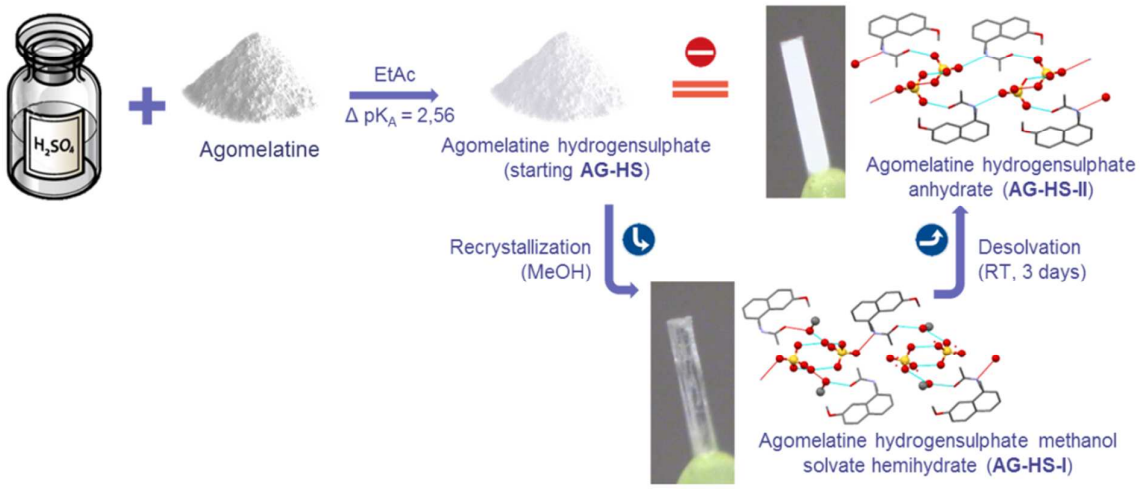

Figure 2 Overview of the formation of hydrogensulfates of AG

The molecular structures of the two AG hydrogensulfates (asymmetric units, H-bonding, molecular packing and a theoretical XRPD compared to experimental XRPD of the starting AG-HS, labeled as AG-HS-II exp., because it is the form it corresponds to) are depicted in Figure 3. AG-HS-I crystallized in the triclinic system with the space group $P\bar{1}$. In its asymmetric unit, it has two molecules of protonated agomelatine, two hydrogensulfate anions, two molecules of methanol and a single water molecule (Figure 3 - a), making it a methanol solvate hemihydrate.

It can be seen that hydrogen bonding system is quite complicated (Figure 3b). However, a basic structural motif is characterized by the two hydrogensulfate homodimeric units in the center that are bridging two AG molecules. There exist two basic variants of this motif depending on the presence or absence of water. Each motif either contains two (right in Figure 3 - b) or none (left in Figure 3 - b) molecules of water. From the structural data, it can be inferred that the H-bonding with the water molecules is stabilizing factor, since their absence leads to the disorder in the hydrogensulfate positions.

AG-HS-II crystallized in the monoclinic system with the space group $P\,2_1$. In the asymmetric unit, it contains a molecule of protonated agomelatine and a hydrogensulfate anion (Figure 3 - e). Hydrogen bonding pattern (Figure 3 - f) is quite similar as in AG-HS-I, but the agomelatine and hydrogensulfate molecules interact directly due to the lack of any solvent. Molecular packing is very similar in both structures (Figure 3 – c, g). In both, we can observe hydrophobic and hydrophilic layers. Interestingly, the symmetry change from triclinic to monoclinic (Table 1) upon the desolvation implies that topotactic rather than single-crystal to single-crystal transformation takes place.[49] Such transition proceeds via nucleation and growth of a new phase (ansolvate), with the crystallites (domains) that are more or less perfectly oriented, simulating the diffraction pattern of a single crystal. This is further evidenced by the lower similarity of the XRPD patterns of the two forms (Figure 3 – d) than would be expected for SCSC.

The traces of the original solvate centrosymmetric structure could be found in the crystal of the ansolvate, because, though having an enantiomorphic space group, it had to be refined as a centrosymmetric racemic twin with the twin matrix of (1 -1 1) and the refined twin ratio of 0.59 : 0.41.

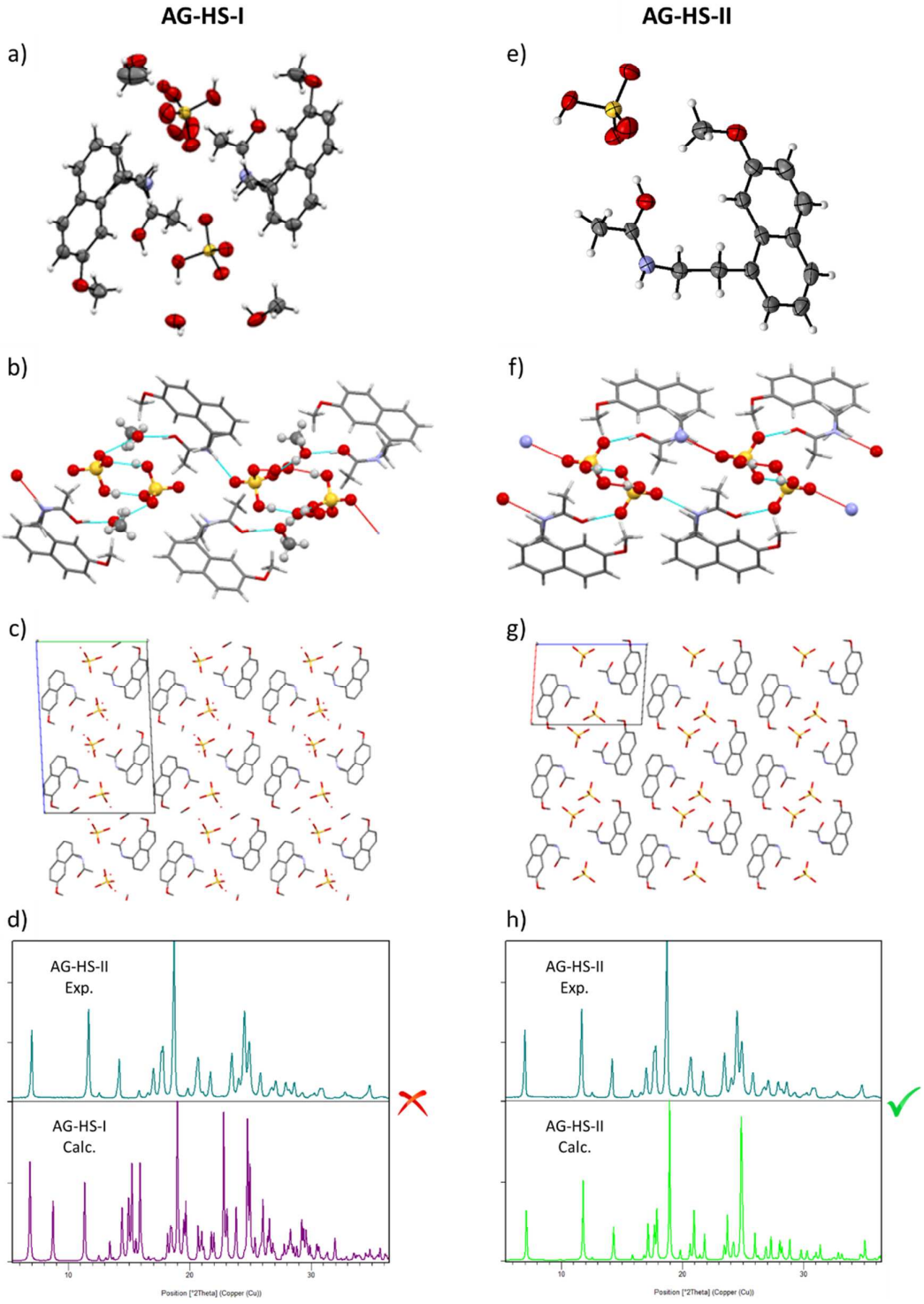

Figure 3 Comparison between agomelatine hydrogensulfates. A MeOH solvate hemihydrate AG-HS-I (a-d) and an ansolvate AG-HS-II (e-h). Asymmetric unit in a, e; H-bonding in b, f; crystal packing in c, g; agreement in the theoretical and experimental XRPD in d, h.

Agomelatine Mesylates

Many aspects of the crystallization of the AG mesylates are similar to AG hydrogensulfates. By crystallization of AG with methansulfonic acid, agomelatine mesylate (AG-MS) is prepared. In analogy with the AG-HS, a single-crystal structure of a solvated form was observed (a monohydrate, AG-MS-I), which did not correspond to the bulk material (Figure 4 – d shows the lack of similarity in the XRPD patterns). Unlike in the case of AG-HS, we were not able to obtain a single-crystal of the anhydrous form (AG-MS-II), neither by recrystallization, nor by SCSC transformation. The crystal structure of the AG-MS-II was determined from the powder X-ray diffraction data. Figure 4h shows the final Rietveld plot and the difference curve.

To verify the structural determination of agomelatine mesylate anhydrate (AG-MS-II) obtained employing powder X-ray diffraction technique, the DFT-D geometry optimization was carried out. The optimization was done in a 2-step way as suggested by J. Streek and M. A. Neumann[50]. First, the geometry of the structure was optimized, followed by the cell parameters optimization. To be able to compare original geometry and DFT-D optimized geometry, Cartesian root-mean-square displacement (RMSCD) as defined in ref.[50] was calculated in Crystal CMP software[51]. The RMSCD values of 0.0524 Å (cell fixed, H-atom excluded) and 0.0753 Å (cell optimized, H-atoms excluded) are both less than 0.25 Å, which is typical for correctly solved structures[50]. Therefore, the structure solution of agomelatine mesylate anhydrate from the XRPD data can be considered as reliable. It should be mentioned that the positions of H atoms obtained by DFT confirmed the salt characteristic of the solid form.

The AG-MS-I crystallized in the triclinic system with the space group $P\bar{1}$. In its asymmetric unit, it has a molecule of protonated agomelatine, a mesylate anion and a single water

molecule (Figure 4a), making it a monohydrate. Hydrogen bonding in AG-MS-I (Figure 4b) can be described as an infinite ladder-like chain.

The AG-MS-II was found to crystallize in the monoclinic system with the space group $P\,2_1/c$. In the asymmetric unit, it contains a molecule of protonated agomelatine and a mesylate anion (Figure 4e). Hydrogen bonding in AG-MS-II (Figure 4f) forms a simple infinite chain with alternating agomelatine and mesylate molecules. As can be seen in Figures 4c, g the hydrophobic and hydrophilic layers can be identified in both AG-MS-I and AG-MS-II. At the same time, the two structures exhibit a completely different molecular packing, which precludes even the possibility of the SCSC transformation.

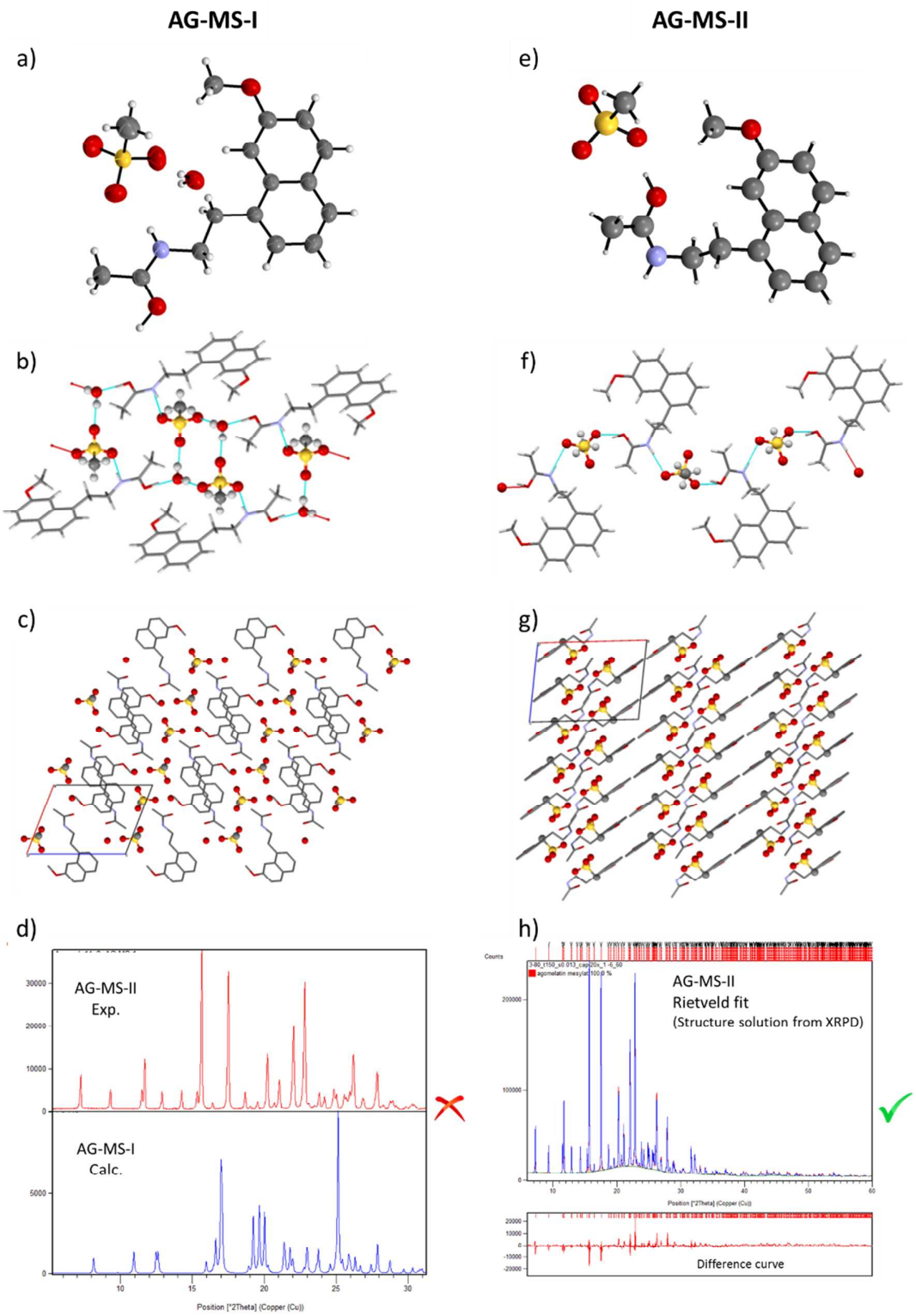

Figure 4 Comparison of agomelatine mesylates. A monohydrate AG-MS-I (a-d) and an anhydrate AG-MS-II (e-h). Asymmetric unit in a, e; H-bonding in b, f; crystal packing in c, g; agreement in the theoretical and experimental XRPD in d, h.

Agomelatine Besylate

AG crystallizes with benzenesulfonic acid (AG-BS) in the orthorhombic system with the space group $P\,2_12_12_1$. In the asymmetric unit (Figure 5a), the structure contains a protonated agomelatine molecule and a besylate anion. Hydrogen bonding involves amidic group of agomelatine and the sulfate group of the besylate anion. They form infinite chains (Figure 5b) and result in hydrophobic and hydrophilic layers in the molecular packing (Figure 5c). The solved crystal structure of AG-BS corresponded to the powder bulk material (Figure 5d). No hydrated or solvated phases of AG besylate were found.

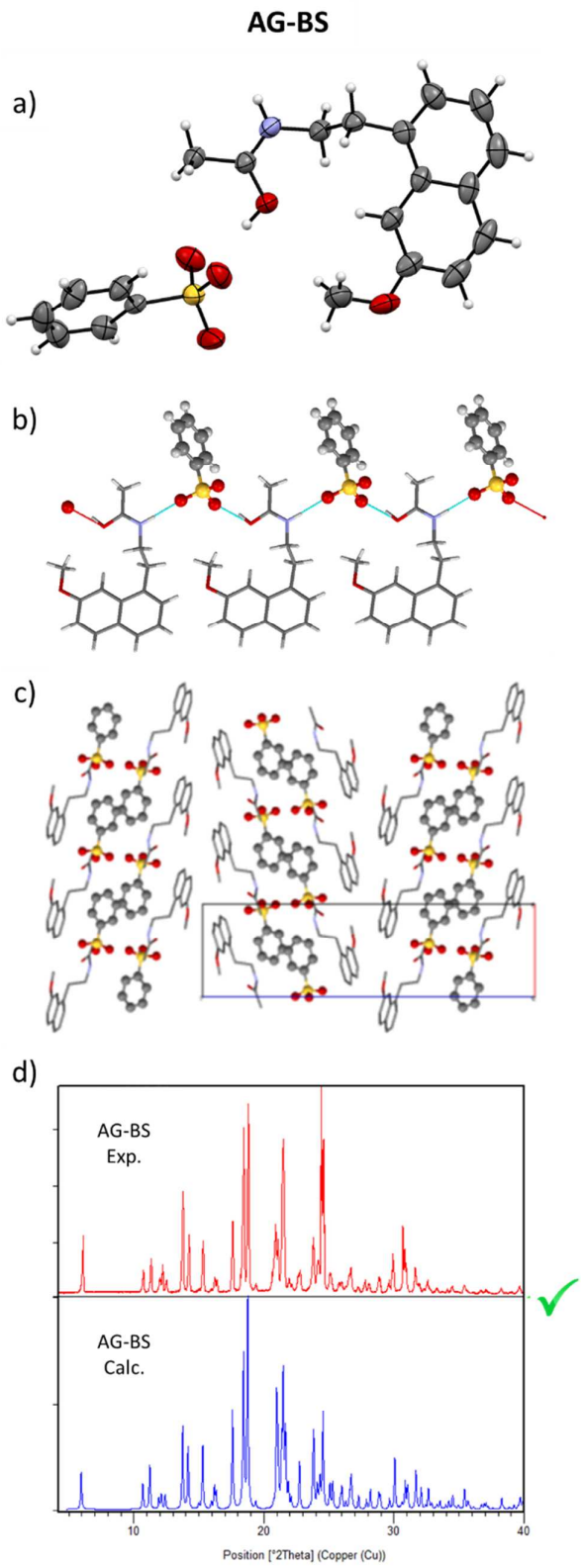

Figure 5 Structural features of agomelatine besylate. Asymmetric unit in a; H-bonding in b; crystal packing in c; agreement in the theoretical and experimental XRPD in d.

Comparison of Agomelatine Crystal Structures

The five new crystal structures of agomelatine were compared with all of the 18 various previously published structures, mostly concentrating on its molecular conformations and crystal packing. A detailed comparison can be found in the Supporting information. Agomelatine was found to exist in three general conformations related to the torsion angle of the side chain (see Figures S2 and S3 in the Supporting Information).

The similarities and differences in the molecular crystal packing were analyzed employing a packing similarity tree diagram. Figure S4 in the Supporting Information shows the diagram for the AG structures calculated by the CrystalCMP software[51].

The structures were generally very dissimilar and mostly, do not form structural types. This lack of similarity is quite unusual, because, when a larger number of crystal structures of the same compound is studied, typically, they are comprised of several 'isostructural' families[3,51–53]. Despite the general lack of similarity, we have found that one of the here presented structures (AG-HS-I) is surprising similar to agomelatine hydriodide trihydrate (Figure 6).

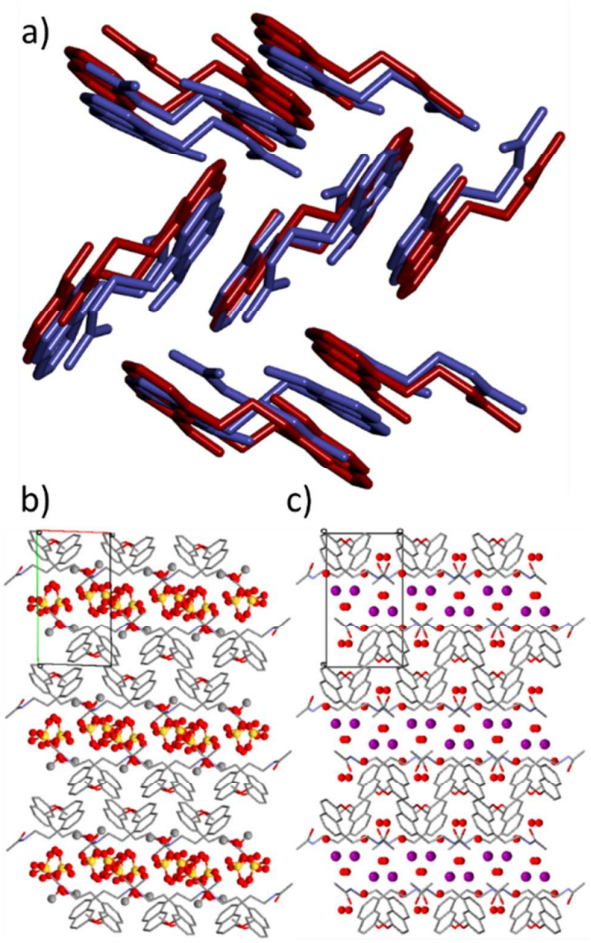

Figure 6 Similar crystal packing of agomelatine molecules in AG-HS-I (b, violet in Figure a) and AG hydriodide trihydrate (c, red in Figure a). Molecular overlay (a) calculated in CrystalCMP.

We find it quite surprising that two structures with such a different composition can have a so similar packing. The sterical end electronic properties of the guest molecules are probably just right to promote the same packing of the agomelatine molecules.

3.2 Ionization of Agomelatine

Although the amidic group can be protonated in the presence of a strong acid, this is quite rare in the solid state and thus only 0.3 % of amides found in the CSD are in a protonated state. Such product of protonation would be expected to be rather unstable (unisolable) or prone to hydrolysis.[54]

In the present study, we have prepared solid forms of AG with various sulfonic acids. In all cases, we have surprisingly obtained the protonated forms of AG, in contrast with the expected co-crystals (co-crystal formation was expected especially with benzensulfonic acid). Therefore, we further complement the data from X-ray crystallography (previous section) with other experimental and theoretical methods in order to provide an additional evidence to support the formation of protonated solid forms. These data are also invaluable in the better understanding of the process of protonation of poorly-ionizable compounds in general.

One of the simplest indications, whether the multi-component solid form is a salt or a co-crystal, is the ΔpK_a rule. It was shown that if the difference between the pK_a of the base and of the acid is greater than 4, the material is most likely a salt. If the ΔpK_a is smaller than -1, the material is most likely a co-crystal[55]. Between these two limits, the formation of both salts and co-crystals can be expected. The probability of a compound being salt or co-crystal is linear and can be calculated as[55]

$$P_{obs}\,(CoCr.,\%) = -17\,\Delta pK_a + 72$$

$$P_{obs}\,(Salt,\%) = 17\,\Delta pK_a + 28$$

In the case of AG sulfonates reported in this work, the ΔpK_a values are in between the limits for all three of them (Table 2) and both forms are therefore possible. As can be seen in Table 2, salt formation might be expected for AG hydrogensulfate, whereas co-crystal formation is more likely to occur for AG besylate. For AG mesylate both forms might have the same probability.

Table 2 The estimated values of ΔpK_a of AG sulfonates and the related probabilities of the forms being either salt or co-crystal.

Form	ΔpK_a*	Co-crystal probability	Salt probability
AG hydrogensulfate	2.7	26 %	74 %
AG mesylate	1.2	52 %	48 %
AG besylate	0.1	70 %	30 %

* All the pK_a values were calculated by ACD Labs as available in SciFinder.

Although, the simple ΔpK_a rule may be indicative in many cases, more advanced methods are usually needed to elucidate the true ionization state of the solid forms. We employed the combination of three methods: analysis of the crystal structures, DFT calculations and solid state NMR.

The X-ray crystallography, provided two independent proofs that agomelatine is protonated on the amidic oxygen (Figure 7a, b). First, utilizing our high-quality data, the position of the acidic hydrogen is evident from the calculated electron density. For agomelatine hydrogensulfate (AG-HS-II, Figure 7a), we can directly observe that the proton is located on the amidic oxygen of agomelatine. Second, the experimentally observed changes in the C-O and C-N bonds clearly indicated the decrease of the bond order in the former and increase of the bond order in the latter, which is perfectly consistent with the protonation of the amidic oxygen (Figure 7b, Table 3).

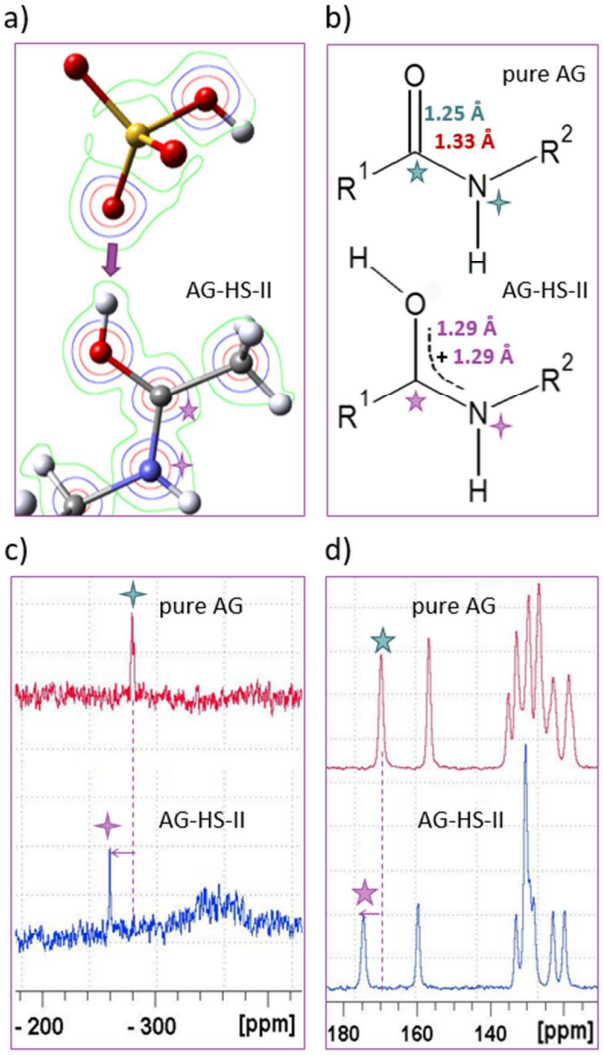

Figure 7 Protonation of agomelatine in AG hydrogensulfate (AG-HS-II) compared with pure AG (polymorph II) as evidenced by SXRD (a, b) and ssNMR (c, d): a) electron density; b) change in amidic bond lengths; c) ^{15}N ssNMR; d) ^{13}C ssNMR. Four- and five-pointed stars indicate N and C atoms in the amidic group, respectively. Green stars indicate data/atoms for pure AG, pink for AG-HS-II.

Table 3 Amidic group bond lengths as found in CSD, extracted from crystal structures of agomelatine and the calculated results.

Form	C-N [Å]	C=O [Å]	(C-N)-(C-O) [Å]
AG - pure polymorph I	1.312	1.223	0.089
AG - pure polymorph II	1.334	1.247	0.087
CSD: neutral amides (median, 96,162 structures)	1.354	1.226	0.128
Calc.: neutral AG	1.36	1.24	0.12
AG hydrogensulfate[a]	1.290	1.289	0.001
AG mesylate[b]	1.302	1.284	0.018
AG besylate	1.291	1.290	0.001
CSD: amide salts (median, 244 *O*-protonated structures)	1.309	1.298	0.011
Calc.: O-protonated AG	1.31	1.32	0.01
Calc.: N-protonated AG	1.58	1.19	0.39

[a] averages of AG-HS-I and AG-HS-II; [b] data corresponding only to AG-MS-I

Further independent evidence was provided by the quantum chemical calculations. The calculated relative pK_a values differ by approximately 8 units: -0.7 for the '*O*-protonated' structure vs. -8.5 for the '*N*-protonated' structure (c.f. Figure S5).

For direct comparison with the experimental bond lengths, the neutral, the '*O*-protonated' and the '*N*-protonated' AG structures were optimized at the BP86/def-TZVP level employing implicit solvation model COSMO (with ε = 6.0 corresponding to the dielectric constant of ethyl acetate). Calculated bond distances are summarized in the **Error! Reference source not found.** above. The calculations clearly show that the protonation of agomelatine leads to the change in the bond orders. Expectedly, the protonation of the oxygen atom leads to a decrease of the bond order of C-O bond (large C-O bond distance), whereas the character of the C-N bond is closer to the double bond. The opposite holds true, when agomelatine is protonated on nitrogen.

The ionization state of agomelatine was also confirmed based on the calculations in periodic (solid state) quantum chemical calculations at the DFT (PBE+D3) level of theory employing the VASP package, v. 5.2 (c.f. Computational Details above). The data are summarized in

Figure 7. All geometry optimizations for AG-BS, AG-MS and AG-HS lead to the exclusive formation of protonated agomelatine. Also, moving on the potential energy surface from salt to co-crystal (i.e. utilizing scan procedure along the O_{AG}–H…O_{acid} with keeping O_{AG}–H bond fixed in each step and with relaxation performed for the rest of the system) we did not observe any other local minimum than the one corresponding to the protonated agomelatine. In fact, the relative energies of co-crystals are several kcal.mol^{-1} higher than the corresponding minima. The biggest difference in the energy of co-crystal and salt is observed for AG-HS system, which is also in accordance with ΔpK_a rule. The relative energies of AG-MS and AG-BS co-crystals are comparable and approximately 5 kcal.mol^{-1} higher than the respective agomelatine salt.

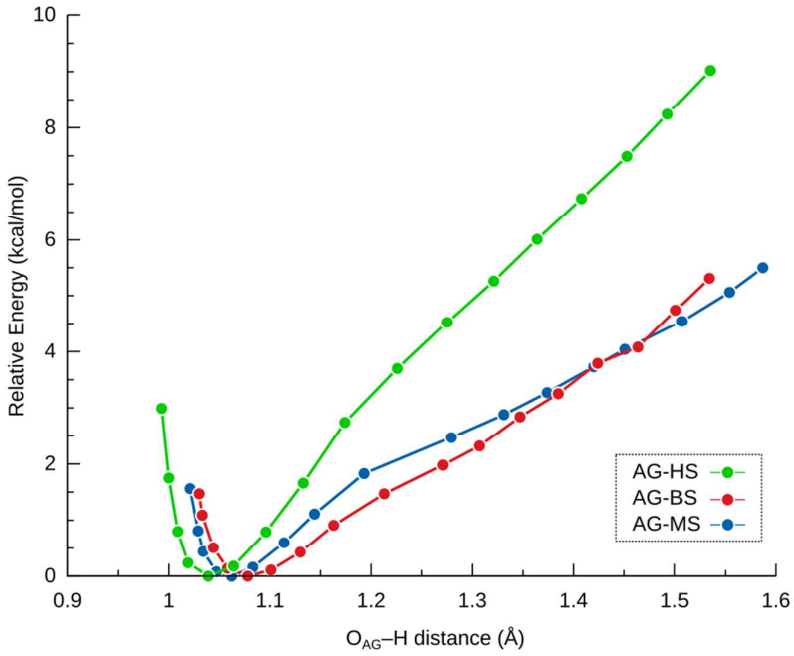

Figure 8 The relative energy of the simulated salt co-crystal continuum for the agomelatine hydrogensulfate (AG-HS), besylate (AG-BS) and mesylate (AG-MS).

Finally, the solid state NMR (ssNMR) was employed to provide further experimental evidence concerning the ionization state of the studied molecules. In Figures 7c, d, an example of the

^{15}N and ^{13}C spectra of AG-HS-II and of pure agomelatine are depicted, whereas all ssNMR data are summarized in Table 4.

Table 4 The chemical shift of amidic C and N in the corresponding ssNMR and compared to pure AG (the average between AG polymorphs I and II).

Solid form	**chemical shift -^{15}N [ppm]**	**Δ ^{15}N (vs. pure AG) [ppm]**	**chemical shift -^{13}C [ppm]**	**Δ ^{13}C (vs. pure AG) [ppm]**
AG hydrogensulfate (AG-HS-II)	-259.50	-21.61	174.60	-3.95
AG mesylate (AG-MS-II)	-253.30	-27.81	176.00	-5.35
AG besylate (AG-BS)	-261.00	-20.11	178.10	-7.45
AG - pure polymorph I	-282.41	-	171.60	-
AG - pure polymorph II	-279.80	-	169.70	-

As can be seen from both Figure 7 and Table 4, the transformation between the two forms - the pure agomelatine forms and their sulfonates - is accompanied by the significant increase/decrease of the chemical shift. Interestingly, the change of the chemical shift of the amidic C and N does not seem to correlate either with the ΔpK_a value or with the difference in the bond lengths in the crystal structures. Moreover, the change of the chemical shift is different and uncorrelated for the ^{15}N and ^{13}C atoms.

In summary, all forms can be clearly described as salts, even though the co-crystal formation was expected for AG besylate (or more precisely, predicted by the ΔpK_a rule). This observation is justified by the crystal structures and packing of AG solid forms, which is more energetically favorable for the molecules in an ionic forms.

3.3 Dissolution

The need to increase solubility and dissolution is often the driving force to search for salts and co-crystals, as they both often offer superior properties compared to the parent compound. Therefore, here we provide the experimental data about intrinsic dissolution rate (IDR) of the agomelatine sulfonates compared to the thermodynamically most stable pure polymorph of

AG, form II. IDR is used for a direct comparison between the speeds of dissolution of different solid phases, without the influence of particle size distribution. It is expressed as the mass dissolved per unit time and area.

The IDR results for AG sulfonates compared to AG form II can be found in Figure 9 and Table S1 and Figure S6 in the Supporting information. We can see that all three salts provide an increase in dissolution. Agomelatine hydrogensulfate dissolved 3.2 times faster than AGII; agomelatine besylate 51.4 times faster and agomelatine mesylate an astonishing 200 times faster.

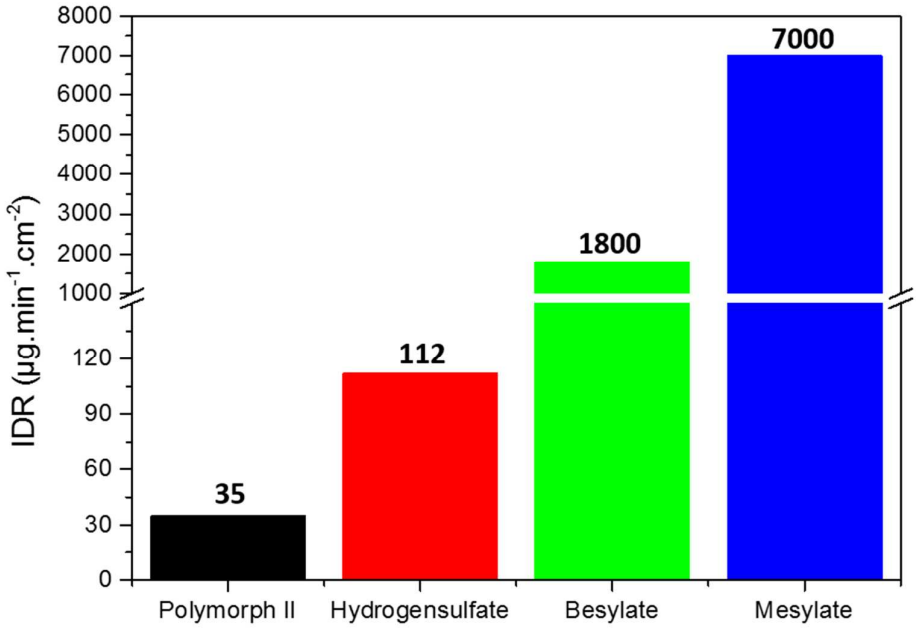

Figure 9 Intrinsic dissolution of agomelatine sulfonates compared to AG polymorph II

We have to note, that the extremely fast dissolution of the last two mentioned samples also effected the precision of the measurement itself. Only several points at the beginning of the dissolution experiments can be considered, because the surface of the sample pellet quickly became uneven. Therefore, the presented values should be taken as tentative. Nevertheless, it is clear that the salt formation increased the dissolution of agomelatine in a significant way.

The highest soluble AG salt found in our work was AG mesylate. As it was described, that the mesylate salts tend to be the most soluble of the amine salts[8], this might suggest, that this trend could apply similarly to the amidic salts.

To rationalize the different dissolution rates of our salts a very recent study[56] can be utilized. In that work, authors reported the dissolution data for 51 salts of methylefedrine and correlated their solubility with other physico-chemical characteristics. A correlation was found between the solubility and melting point of the salt and also between melting point of the salt and melting point of the parent acid. However, a pronounced correlation was only observed for salts with similar packing of the API cation. This strongly implies, that the packing structure plays a significant role in determining solubility and other properties of the salts. From Table 5, there is an evident correlation between the melting points of the salts and their dissolution. This corresponds to the expected trends, because melting point is an indicator of thermodynamic stability and low stability generally means high solubility. In contrast to the observations made in the ref.[56], we did not find any correlation between the melting point of the parent acid and the melting point of the salt. However, this apparent controversy is in agreement with authors' statement that these correlations were good only for isostructural groups. As shown in the section 3.1, the sulfonates of AG do not have a similar packing which further corroborates the notion, that the crystal structure plays the key role in determining the physico-chemical properties.

Table 5 Comparison of dissolution rate and melting point of agomelatine sulfonate salts and of melting points of the parent acids.

Solid form	**IDR** $\mu g\ min^{-1}\ cm^{-2}$	$T_{m,\ salt}$ °C	$T_{m,\ acid}$ °C
AG hydrogensulfate	112	152.5	10[57]
AG mesylate	7000	99.8	18[58]
AG besylate	1800	135.7	46[59]

From the crystal engineering point of view, an interesting question is how the salts are compared to the co-crystals. In the work of Yan et al.[22], we can find the results of powder dissolution of four AG co-crystals. The dissolution rate increase was between 2.2 to 4.7 times compared to AGII. Even though, the method of analysis was not identical to ours (intrinsic dissolution rate vs. powder dissolution rate), we are able to make a meaningful comparison based on the magnitude of dissolution increase compared to the most stable polymorph of AG. AG hydrogensulfate (IDR increase of 3.2) has presumably a similar dissolution rate to the co-crystals, but the other two salts, AG mesylate and AG besylate (IDR increase of ~ 200 and ~ 50, respectively), dissolve much faster.

4 CONCLUSIONS

In this work, we reported three novel sulfonate salts of agomelatine – an important pharmaceutical. These included a hydrogensulfate, a mesylate and a besylate and for two of them, their respective solvated forms. The crystal structures of all solid forms were determined employing the single-crystal or powder X-ray diffraction data. The crystal structure of agomelatine hydrogensulfate ansolvate was obtained via topotactic transformation from a solvate single-crystal of this form. The structures were compared to the previously described structures of agomelatine and it was discovered that, as opposed to most other organic crystalline compounds, agomelatine does not easily form isostructural families.

Four methods – simplistic ΔpK_a rule, X-ray crystallography, quantum chemical calculations, and ssNMR measurements - were used to prove that the forms are indeed salts. They all unambiguously pointed to the protonation of the amide oxygen. This is further supported by the experiments demonstrating the increase in the dissolution of agomelatine (up to a factor of ~200). This value is much greater than the values reported in the literature for the co-crystals (~5), which makes our approach attractive for practical utilization. Therefore, to improve

compound's solubility, a salt formation (as an alternative route to co-crystals) should be also explored even for the poorly-ionizable amidic compounds.

ACKNOWLEDGMENT

We would like to acknowledge the Solid State department of Zentiva, k.s. for the materials and all the help provided. This work was supported by the Czech Science Foundation (GA ČR) projects, Grant Nos. 17-23196S and 16-10035S. JK acknowledges support from the Charles University through the Primus program and computational resources provided by the IT4Innovations National Supercomputing Center (project of the Ministry of Education, Youth, and Sports for large infrastructures for research, experimental development, and innovations, LM2015070). For the measurement on PANanalytical Empyrean diffractometer, we would like to acknowledge Jan Rohlíček from Institute of Physics of the Czech Academy of Sciences.

ASSOCIATED CONTENT

The equilibrium geometries of all studied compounds including the primary energetic data from quantum chemical calculations, Figures S1-S6, high-quality figure of the final Rietveld plot for agomelatine mesylate anhydrate, comparison of agomelatine crystal structures with the comparison of conformations, statistical distribution of the side chain torsion angles and packing similarity tree diagram, primary data from intrinsic dissolution rate and the calculated values. This information is available free of charge via the Internet at http://pubs.acs.org/.

AUTHOR INFORMATION

Corresponding Author

* E-mail: eliska.skorepova@vscht.cz

Author Contributions

The manuscript was written through contributions of all authors. All authors have given approval to the final version of the manuscript.

REFERENCES

(1) Hilfiker, R. *Polymorphism*; John Wiley & Sons, 2006.
(2) Blagden, N.; de Matas, M.; Gavan, P. T.; York, P. *Adv. Drug Deliv. Rev.* **2007**, *59*, 617–630.
(3) Skořepová, E.; Hušák, M.; Čejka, J.; Zámostný, P.; Kratochvíl, B. *J. Cryst. Growth* **2014**, *399*, 19–26.
(4) Khadka, P.; Ro, J.; Kim, H.; Kim, I.; Kim, J. T.; Kim, H.; Cho, J. M.; Yun, G.; Lee, J. *Asian J. Pharm. Sci.* **2014**, *9*, 304–316.
(5) Thakuria, R.; Nangia, A. *Cryst. Growth Des.* **2013**, 130628120410008.
(6) Almarsson, Ö.; Zaworotko, M. J. *Chem. Commun.* **2004**, No. 17, 1889.
(7) Stephenson, G. A.; Aburub, A.; Woods, T. A. *J. Pharm. Sci.* **2011**, *100*, 1607–1617.
(8) Elder, D. P.; Delaney, E.; Teasdale, A.; Eyley, S.; Reif, V. D.; Jacq, K.; Facchine, K. L.; Oestrich, R. S.; Sandra, P.; David, F. *J. Pharm. Sci.* **2010**, *99*, 2948–2961.
(9) Good, D. J.; Rodríguez-Hornedo, N. *Cryst. Growth Des.* **2009**, *9*, 2252–2264.
(10) Mittapalli, S.; Mannava, M. K. C.; Khandavilli, U. B. R.; Allu, S.; Nangia, A. *Cryst. Growth Des.* **2015**, *15*, 2493–2504.
(11) Sanphui, P.; Tothadi, S.; Ganguly, S.; Desiraju, G. R. *Mol. Pharm.* **2013**, *10*, 4687–4697.
(12) Grifasi, F.; Chierotti, M. R.; Gaglioti, K.; Gobetto, R.; Maini, L.; Braga, D.; Dichiarante, E.; Curzi, M. *Cryst. Growth Des.* **2015**, *15*, 1939–1948.
(13) Andrieux, J.; Houssin, R.; Yous, S. L. de C. S.; Guardiola, B.; Lesieur, D. Naphthalene derivatives, procedure for their preparation and pharmaceutical compositions containing them. EP0447285 A1, September 18, 1991.
(14) Li, G.; Zhou, H.; Jiang, Y.; Keim, H.; Topiol, S. W.; Poda, S. B.; Ren, Y.; Chandrasena, G.; Doller, D. *Bioorg. Med. Chem. Lett.* **2011**, *21*, 1236–1242.
(15) Boutin, J. A.; Audinot, V.; Ferry, G.; Delagrange, P. *Trends Pharmacol. Sci.* **2005**, *26*, 412–419.
(16) Delagrange, P.; Boutin, J. A. *Chronobiol. Int.* **2006**, *23*, 413–418.
(17) Calabrese, J. R.; Guelfi, J. D.; Perdrizet-Chevallier, C.; Agomelatine Bipolar Study Group. *Bipolar Disord.* **2007**, *9*, 628–635.
(18) Stein, D. J.; Ahokas, A. A.; de Bodinat, C. *J. Clin. Psychopharmacol.* **2008**, *28*, 561–566.
(19) Tinant, B.; Declercq, J. P.; Poupaert, J. H.; Yous, S.; Lesieur, D. *Acta Crystallogr. C* **1994**, *50*, 907–910.
(20) Zheng, S.-L.; Chen, J.-M.; Zhang, W.-X.; Lu, T.-B. *Cryst. Growth Des.* **2011**, *11*, 466–471.
(21) Holaň, J.; Skořepová, E.; Heraud, L.; Baltes, D.; Rohlíček, J.; Dammer, O.; Ridvan, L.; Štěpánek, F. *Org. Process Res. Dev.* **2016**, *20*, 33–43.
(22) Yan, Y.; Chen, J.-M.; Geng, N.; Lu, T.-B. *Cryst. Growth Des.* **2012**, *12*, 2226–2233.
(23) Prohens, R.; Barbas, R.; Portell, A.; Font-Bardia, M.; Alcobé, X.; Puigjaner, C. *Cryst. Growth Des.* **2016**, *16*, 1063–1070.
(24) Skořepová, E.; Hušák, M.; Ridvan, L.; Tkadlecová, M.; Havlíček, J.; Dušek, M. *CrystEngComm* **2016**, *18*, 4518–4529.

(25) Perumalla, S. R.; Sun, C. C. *CrystEngComm* **2013**, *15*, 8941–8946.
(26) Manallack, D. T. *Perspect. Med. Chem.* **2007**, *2007*, 25–38.
(27) Bordwell, F. Bordwell pKa Table http://www.chem.wisc.edu/areas/reich/pkatable/index.htm (accessed Jul 18, 2017).
(28) Buist, A. R.; Kennedy, A. R.; Shankland, K.; Shankland, N.; Spillman, M. J. *Cryst. Growth Des.* **2013**, *13*, 5121–5127.
(29) Nanubolu, J. B.; Sridhar, B.; Ravikumar, K. *CrystEngComm* **2012**, *14*, 2571–2578.
(30) *CrysAlisPro*; Oxford Diffraction, 2002.
(31) *SIR92*; J. Appl. Cryst., 1994.
(32) Palatinus, L.; Chapuis, G. *J. Appl. Crystallogr.* **2007**, *40*, 786–790.
(33) Betteridge, W. *CRYSTALS*; 2003.
(34) Petricek; Palatinus. *Jana2006*; Institute of Physics: Prague, The Czech Republic.
(35) Spek, A. L. *Acta Crystallogr. D Biol. Crystallogr.* **2009**, *65*, 148–155.
(36) Cooper, R. I.; Gould, R. O.; Parsons, S.; Watkin, D. J. *J. Appl. Crystallogr.* **2002**, *35*, 168–174.
(37) *Mercury*; CCDC, 2007.
(38) *Discovery Studio*; Accelrys, Inc.
(39) *X'PERT HighScore Plus*; PANanalytical BV, 2009.
(40) David, W. I. F.; Shankland, K.; van de Streek, J.; Pidcock, E.; Motherwell, W. D. S.; Cole, J. C. *J. Appl. Crystallogr.* **2006**, *39*, 910–915.
(41) Boultif, A.; Louër, D. *J. Appl. Crystallogr.* **2004**, *37*, 724–731.
(42) Clark, S. J.; Segall, M. D.; Pickard, C. J.; Hasnip, P. J.; Probert, M. I. J.; Refson, K.; Payne, M. C. *Z. Für Krist. - Cryst. Mater.* **2005**, *220*.
(43) Kelly, C. P.; Cramer, C. J.; Truhlar, D. G. *J. Phys. Chem. B* **2006**, *110*, 16066–16081.
(44) Kresse, G.; Furthmüller, J. *Comput. Mater. Sci.* **1996**, *6*, 15–50.
(45) Kresse, G.; Joubert, D. *Phys. Rev. B* **1999**, *59*, 1758–1775.
(46) Perdew, J. P.; Burke, K.; Ernzerhof, M. *Phys. Rev. Lett.* **1996**, *77*, 3865–3868.
(47) Grimme, S.; Antony, J.; Ehrlich, S.; Krieg, H. *J. Chem. Phys.* **2010**, *132*, 154104.
(48) Grimme, S.; Ehrlich, S.; Goerigk, L. *J. Comput. Chem.* **2011**, *32*, 1456–1465.
(49) Clarke, J. B.; Hastie, J. W.; Kihlborg, L. H. E.; Metselaar, R.; Thackeray, M. M. *Pure Appl. Chem.* **1994**, *66*, 577–594.
(50) van de Streek, J.; Neumann, M. A. *Acta Crystallogr. Sect. B Struct. Sci. Cryst. Eng. Mater.* **2014**, *70*, 1020–1032.
(51) Rohlíček, J.; Skořepová, E.; Babor, M.; Čejka, J. *J. Appl. Crystallogr.* **2016**, *49*, 2172–2183.
(52) Sládková, V.; Skalická, T.; Skořepová, E.; Čejka, J.; Eigner, V.; Kratochvíl, B. *CrystEngComm* **2015**, *17*, 4712–4721.
(53) Zvoníček, V.; Skořepová, E.; Dusek, M.; Babor, M.; Žvátora, P.; Soos, M. *Cryst. Growth Des.* **2017**.
(54) Holman, R. W. *J. Chem. Educ.* **1995**, *72*, A151.
(55) Cruz-Cabeza, A. J. *CrystEngComm* **2012**, *14*, 6362–6365.
(56) S. de Moraes, L.; Edwards, D.; Florence, A. J.; Johnston, A.; Johnston, B. F.; Morrison, C. A.; Kennedy, A. R. *Cryst. Growth Des.* **2017**, *17*, 3277–3286.
(57) Macy, R. *Chem. Corps J.* **1947**, *1*, 36–38.
(58) Tan, B.-H.; Yoshio, M.; Kato, T. *Chem. - Asian J.* **2008**, *3*, 534–541.
(59) Qureshi, Z.; Deshmukh, K.; Jagtap, S.; Nandurkar, N.; Bhanage, B. *Ultrason. Sonochem.* **2009**, *16*, 308–311.

For Table of Contents Use Only

Increase in Solubility of "Poorly-Ionizable" Pharmaceuticals by Salt Formation. A Case of Agomelatine Sulfonates.

Eliška Skořepová, Daniel Bím, Michal Hušák, Jiří Klimeš, Argyro Chatziadi, Luděk Ridvan, Tereza Boleslavská, Josef Beránek, Pavel Šebek, Lubomír Rulíšek

TABLE OF CONTENT GRAPHICS

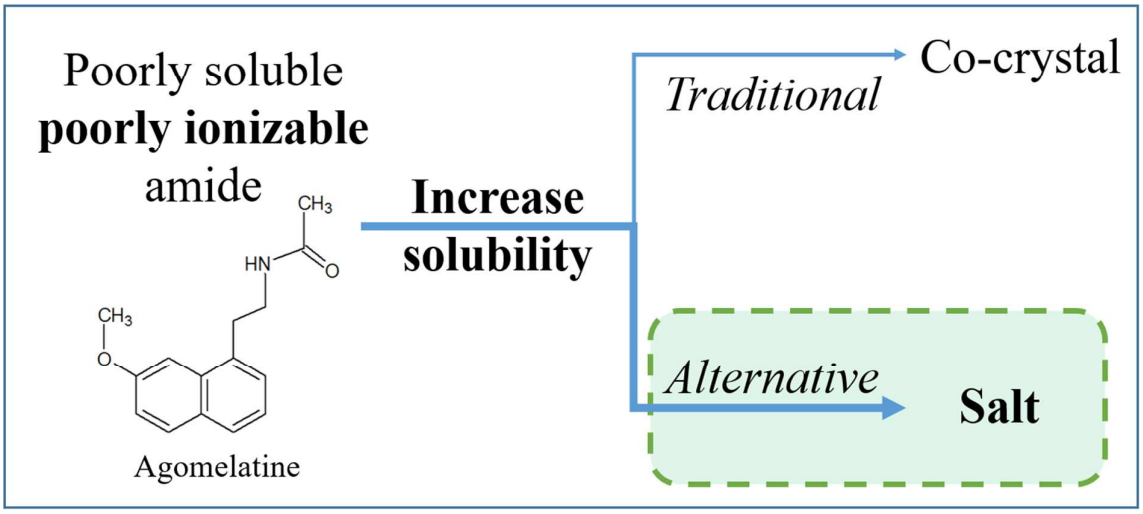

SYNOPSIS

We present three novel sulfonate salts of agomelatine – a hydrogensulfate, a mesylate and a besylate and for two of them, their respective solvated forms. All crystal structures have been solved and their salt character was confirmed by solid state NMR measurements and DFT calculations. By sulfonate salt formation, up to ~200-times faster dissolution of agomelatine was achieved.